Nat Hazards
DOI 10.1007/s11069-014-1516-6

ORIGINAL PAPER

The measurement of wind erosion through field survey and remote sensing: a case study of the Mu Us Desert, China

Yaojie Yue · Peijun Shi · Xueyong Zou · Xinyue Ye · A-xing Zhu · Jing-ai Wang

Received: 10 May 2014 / Accepted: 4 November 2014

Abstract The measurement of wind erosion is not only important to understand wind erosion itself, but also an important scientific step in efforts to reverse the process of desertification. This study develops a model that predicts sand transport flux at pixel level based on the quantitative relationship between remotely sensed vegetation coverage and observed sand transport rate data. The data were collected from field surveys in the sandy area of Yuyang County, which is located in the Mu Us Desert. The study found that the sand transport flux was 9,643 kilograms per meter annually ($kga^{-1}\ m^{-1}$) for a mobile dune, 6,394 $kga^{-1}\ m^{-1}$ for a semi-mobile dune, 2,634.5 $kga^{-1}\ m^{-1}$ for bare cultivated land, and 127.7 $kga^{-1}\ m^{-1}$ for a semi-fixed dune. Using the sand flux derived by our model, the wind erosion modulus in the Yuyang sandy area was found to be 1,673.18 tons per square kilometer annually [$ta^{-1}\ (km^2)^{-1}$] in 1986, 1,568.10 in 1996, and 1,685.04 in 2005. Mean vegetation coverage in the sandy area of Yuyang in 1986, 1996, and 2005 was 42.39, 48.07, and 48.03 %, respectively, indicating that overall, vegetation coverage

Y. Yue · J. Wang (✉)
School of Geography, Beijing Normal University, Beijing 100875, China
e-mail: jwang@bnu.edu.cn

Y. Yue · A.-x. Zhu
Department of Geography, University of Wisconsin-Madison, Madison, WI 53706, USA

Y. Yue · P. Shi · X. Zou · J. Wang
State Key Laboratory of Earth Surface Processes and Resource Ecology, Beijing Normal University, Beijing 100875, China

X. Ye
Department of Geography, Kent State University, Kent, OH 44242, USA

A.-x. Zhu
Jiangsu Center for Collaborative Innovation in Geographical Information Resource Development and Application and School of Geography, Nanjing Normal University, Nanjing, China

A.-x. Zhu
State Key Laboratory of Resources and Environmental Information System, Institute of Geographic Sciences and Natural Resources Research, Chinese Academy of Sciences, Beijing, China

Published online: 30 January 2015

increased in the region, while decreasing in some areas, and that the vegetation coverage incensement failed to reduce the quantity of regional wind erosion. This sand flux retrieval method has the potential for successful application in other, similar areas.

Keywords Wind erosion · Quantitative retrieval model · Field survey · Remote sensing · Mu Us Desert

1 Introduction

Drylands cover about 41 % of Earth's land surface (Kassas 1995; GLP 2005; MEA 2005; Reynolds et al. 2007), and these territories are prone to desertification (Kassas 1995). It has been estimated that about 25 % of dryland areas around the world are affected by desertification (D'Odorico et al. 2013). Reduced vegetation cover and increased wind energy usually exacerbate sand transport (Wang and Zhu 2001; Wang et al. 2005a, b, 2006; D'Odorico et al. 2013). Soil erosion caused by wind is considered to be the primary cause of desertification in these regions (Chen et al. 1994; Dong et al. 2000; Wang et al. 2008). The scale of soil erosion has thus created an urgent need for effective estimations of wind erosion in drylands as a step in easing the trend of desertification. The quantitative measurement of wind erosion is in this way central to both the scientific study of wind erosion (Toy et al. 2002; Stroosnijder 2005) and the formulation of a wind erosion control plan to address desertification globally.

While remote sensing data are particularly suitable for observing different scales of wind erosion, we also needed to overcome the gaps in directly quantifying wind erosion from the remote sensing data. Ackerman (1997) suggested that MODIS images are useful for detecting and tackling dust storm events. Zheng et al. (2001), Yan et al. (2002), and Xiong et al. (2002) studied the properties of dust storms in China and East Asia and found that remote sensing data can be applied not only to monitor the dust source and transport route, but also to extract dust quantity. Prospero et al. (2002) examined the distribution of dust sources globally using the NIMBUS 7 Total Ozone Mapping Spectrometer (TOMS) aerosol index over a 13-year period (1980–1992), identifying the world's largest and most persistent dust sources. Gabor and Jozsef (1998) measured the eroded and the accumulated quantity of sand on a weekly basis using 1-m stakes beside a 50-m by 100-m parcel, and identifying territories endangered by wind erosion using the vegetation greenness index and the soil wetness index. With the support of remote sensing and GIS, Zhang et al. (2002) constructed a wind erosion dynamic index using wind speed, soil dryness, NDVI, soil texture, and the slope of the land surface as input factors to reflect the capacity for soil erosion by wind in China. More recently, remote sensing has been used successfully in wind erosion risk mapping (Reiche et al. 2012) and oil erosion simulation (Wang et al. 2014). But these studies did not develop methods for estimating annual sand transport flux. The ability to predict regional wind erosion at pixel level has yet to be achieved. One reason is that the studies have not collected data through field observations to link with remotely sensed data and generate the sand transport flux. There is, however, a method that can combine wind erosion ground measurements with inexpensive and intensively sampled remotely sensed data in order to map net soil transport flux over very large areas.

In order to take advantage of remote sensing and field survey data to predict regional soil wind erosion, Chappell (1998) mapped the ^{137}Cs-derived net soil flux using the co-kriging method in southwest Niger, with the support of SPOT data. However, the correlation

between the SPOT bands and net soil flux was so poor that a linear regression model could not be established. Liu (1999) established different formulas for wind velocity and the transport rate of sand drift on different types of land surfaces, based on field observations of wind erosion and the interpretation of TM images. His study focused primarily on dunes and bare lands, however, and did not take farmland into account. Although the method proposed by Chappell (1998) and Liu (1999) did not have the ability to derive sand flux from remote sensing data, their work does provide a strong basis for further investigating the combination of ground measurements with inexpensive, intensively sampled and remotely sensed data to map net soil flux over very large areas. We therefore hypothesized that remote sensing data would be helpful in determining long-term wind erosion on a regional scale.

The primary goal of this paper was to develop a quantitative retrieval model of sand transport rate on a regional scale, based on ground measurements and remote sensing data. To do this, we first identified the scientific hypotheses and data processing necessary to construct the model and then selected the sandy area of Yuyang County in the Mu Us Desert in China as a case study in which to evaluate it. Results are discussed and compared with previous studies.

2 Data and methods

2.1 Study area and remote sensing data

In China, drylands cover an area of more than 1.6 million km^2 (Zhu et al. 1980; Zhu and Chen 1994; Wang et al. 2006, 2008). Yuyang County, located in the Mu Us Desert in central-northern China (38°N–39°N and 108°E–110°E, see Fig. 1), is in a semiarid and continental climate zone. This area is characterized by dry and windy weather during spring, which can cause severe wind erosion and frequent dust storm events that occur at a rate of 8–13 days per year (Wang et al. 2005b).

The remote sensing data used in this study came from thematic mapper (TM) images with a spatial resolution of 30 m. Three periods (June to August) of TM images in 1986, 1996, and 2005 were selected to represent vegetation coverage during the 1980s, 1990s, and 2000s, respectively. We used the TM images to retrieve the normalized deviation vegetation index (NDVI), which is linked to changes in vegetation coverage. A geometric correction was performed using the ground control points obtained using Mobile Mapper GPS, which provides a position accuracy of less than 1 m or less than half a pixel. All the corrected images were registered to the Universal Transverse Mercator (UTM) projection with a WGS84-coordinate system.

2.2 Soil wind erosion measurement

According to Stroosnijder (2005), erosion measurements should not be replaced with the application of erosion prediction technology. But a paucity of reliable empirical data has rendered erosion measurements nearly unavailable. Field soil wind erosion measurements are important in this study because they are the basis for our experimental wind erosion prediction model. The field experiments included measurements of the sand transport rate (q), wind speed and direction (2 m AGL, U_2), and vegetation coverage (see Sect. 2.3).

Our field observations revealed that for a moving dune and exposed farmland, sand flow occurs once wind speed reaches 4 m $\times$ s^{-1} at 2 m height. The threshold wind velocity for semi-fixed sand dunes was 6 m/s, due to the increase in vegetation cover, while it was 10 m $\times$ s^{-1} for fixed dunes. Many studies have shown that wind erosion does not always

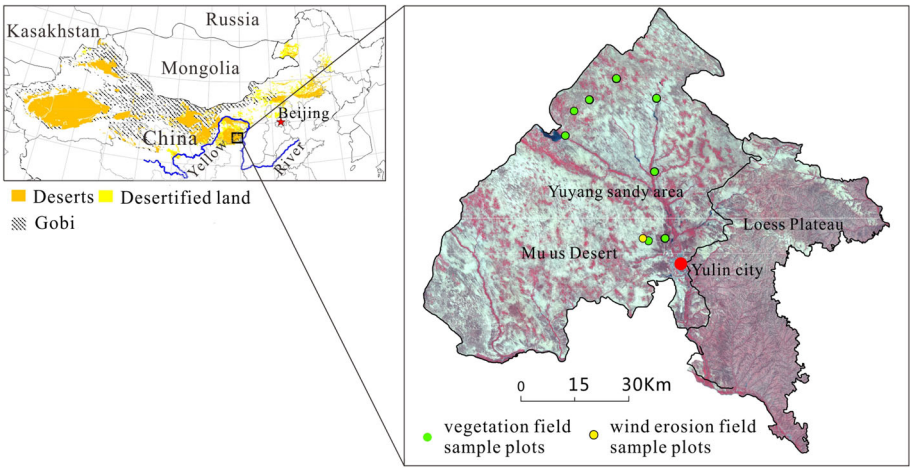

Fig. 1 Location of Yuyang County and the distribution of field sample plots

occur when the vegetation coverage is over 60 % (Dong et al. 1996; Huang et al. 2001). To account for this, the wind erosion field survey sample plots were primarily established on five land surfaces: barren arable land, high vegetation coverage grassland (usually fixed sand dunes), middle vegetation coverage grassland (semi-fixed sand dunes), low vegetation coverage grassland (semi-mobile sand dunes), and mobile dunes. The q and U_2 were continuously observed for the following five types of land cover: bare farmland, fixed sand dunes (A1), semi-fixed sand dunes (A2), semi-mobile sand dunes (A3), and mobile sand dunes (A4). Changhanjie village, which is located in the heart of the Yuyan sandy area, was selected as the observation site through field survey and TM image interpretation. The aeolian landforms and land-use types are typical of the area. Three repetitions (three sample plots) for each land surface type were set up. The observations started in March and lasted until June in both 2006 and 2007. In addition, daily wind speed and direction data (10 m AGL, U_{10}) were acquired for every 6-h period from 1951 to 2003 from the Yulin meteorological station.

The method and equipment used are described by Zobeck et al. (2003). With respect to the q measurement, an anemometer was set at a height of 2 m for recording the mean wind speed at 1-min interval. Four fixed, vertical sand collectors, which were 60 cm high, were set up at the center of each of the sample plots and were placed above ground level, in the hatch face sand flow direction. In addition, wind erosion samples were collected only when the wind speed continuously exceeded the threshold wind velocity. The time of collection was always 5–10 min, according to the sand flow intensity.

Based on Wu (1987), the sand transport rate q for any of the underlying surface for single wind erosion observation can be calculated using Eq. (1),

$$q = \frac{s}{w \times t}, \tag{1}$$

where s is the weight of sand samples, w is the width of the sand entrance in the vertical sand collectors, and t is the observation time.

On the other hand, as a result of wind blown on soil, q also can be seen as a function of wind speed. So, if adequate q and corresponding wind speed data are collected, a regression analysis between q and the corresponding wind speed (U_2) can lead to an empirical formula with the general form of:

$$q_i = f(U_2), \tag{2}$$

where q_i is the sand transport rate of a certain underlying surface at a certain wind speed (U_2). For the purpose of using wind speed data provided by the meteorological station (U_{10}), we used the formula $U_2 = 0.77\ U_{10}$ (Liu 1999) to convert the wind speed. Therefore, the function between q and U_{10} is

$$q_i = f(0.77U_{10}), \tag{3}$$

where q_i is the sand transport rate of a certain underlying surface at a certain wind speed (U_{10}), and U_{10} is the self-recording wind speed at a weather station with a height of 10 m. There are many theoretical and empirical formulas for calculating the sand transport rate (Bagnold 1941; Kuhlman 1958; Owen 1964), but, as discussed below, we found that a new empirical equation was required to fit our data.

Wu (1987) defined sand discharge (Q) as the amount of sand transport for a certain wind direction through a unit width on the land, mean sand transport flux (mean Q) as the summation of Q for all of the wind directions. We can calculate Q_i according to following formula:

$$Q_i = \Sigma q_i \times T_i, \tag{4}$$

where Q_i is the Q of any underlying surface at a certain wind direction when the wind speed exceeds the threshold, q_i is the sand transport rate at a certain wind speed with a certain underlying surface, T_i is the duration for a different threshold wind velocity and data that we can obtain from the weather station. Finally, we can calculate mean Q,

$$\text{Mean } Q = \sum (Q_i \times \sin\theta), \tag{5}$$

where θ is the wind angle.

2.3 Measurement of vegetation coverage

Vegetation coverage was measured for two reasons: (1) to establish a relationship between q and observational vegetation coverage and (2) to establish a link between observational vegetation coverage and NDVI from TM imagery. The vegetation coverage was observed across the sandy area of Yuyang County on nearly 180 sample plots (Fig. 1).

The field-surveyed vegetation coverage could be measured by using high-precision and high-efficiency digital photography (Ackerman 1997; Zhou et al. 1998; Stroosnijder 2005; Chen et al. 2006). For this study, we used a Pentax A20 digital camera as the observing instrument and fixed it at 3 m above the surface. By using differential GPS, we could perform ground photography and GPS positioning simultaneously to ensure the accuracy of the location of the measurements and the shape of the area sampled. At the same time, the size of each sample plot was set to 30 m $\times$ 30 m, which is the same as the pixel size of the TM image. In each quadrant, at intervals of 15 m along the edge of the sample plot and at the diagonal intersection points, we set a measurement point, for a total of nine measurement points. Each point was measured by photographs taken from four vertical directions, so each sample had a total of 36 digital photographs (see Fig. 2).

The following process was used to obtain sample area vegetation coverage through digital photographs (Xie et al. 2008): first, the true-color photograph was transferred to a two-valued photograph to distinguish the vegetation and non-vegetation areas; second, the vegetation coverage for each single photograph was calculated through the recursive search algorithm

and then via the arithmetic average to obtain the vegetation coverage for every measurement point and sample plot. After the removal of overlapping regions, the observation area was 11.91 m^2 for each photograph when the camera was at 3 m height with focal length at 7.9 mm, and the average observation area for each measurement point was 24–26 m^2, so the observation area of nine measurement points accounted for 26.11 % of the sample area.

Usually, vegetation coverage over a large area can be calculated by constructing an empirical model based on a regression of field-surveyed vegetation coverage and the corresponding vegetation index. NDVI, which detects a wide range of vegetation and has good adaptability in terms of phase and space, is the most widely adopted vegetation index. NDVI can be affected by many factors, however, such as soil, moisture, and canopy structure. But, because the vegetation in the Yuyang sandy area is relatively simple with low biomass, its distribution is relatively concentrated, so the boundary of vegetation and bare sand is clear, and NDVI is able to reflect the area's distribution and vegetation coverage. At the same time, vegetation in this area is mostly semi-shrub grass, so coverage can be measured accurately using a digital camera suspended at 3 m. Hence, it is reliable to estimate regional vegetation coverage by constructing an empirical model from a regression of field-surveyed vegetation coverage and corresponding NDVI, as represented by Eq. 6:

$$\mathrm{NDVI} = \frac{(\rho_{\mathrm{NIR}} - \rho_{\mathrm{R}})}{(\rho_{\mathrm{NIR}} + \rho_{\mathrm{R}})} \tag{6}$$

In the equation, ρ_{NIR} represents the near-infrared reflectivity, and ρ_{R} represents the red-band reflectivity.

The key process for constructing an empirical model is to then construct a spatial link between the NDVI pixel values and the corresponding field-observed vegetation coverage. Although the sample plot was set to the same size as the TM pixel, the two did not completely overlap in space. For this reason, they could not be overlaid exactly to match the values of NDVI and the corresponding observed vegetation coverage. We did not adopt sample plot polygons, but did adopt the sample points to overlay with NDVI pixels, allowing us to count out the number of observation points that fall within each pixel. A database was then constructed by matching average vegetation coverage estimated from all the observation points within each pixel and the corresponding NDVI, respectively. Based on the database, we completed a polynomial regression using the least squares method and established the vegetation coverage calculation model. This model uses a cubic polynomial function, and its equation is as follows:

$$\mathrm{VC} = a + b\mathrm{NDVI} + c\mathrm{NDVI}^2 + d\mathrm{NDVI}^3 \tag{7}$$

In this function, NDVI is calculated by Eq. 6, and a, b, c, d are fitting coefficients.

Because the model was established from field survey data and NDVI, it had no ability to relate to historical remote sensing data by inversion, but the same remote sensing data obtained under similar atmospheric and ground conditions were comparable, and the vegetation index obtained through the same model was also comparable. We could therefore use the current inversion results as a reference image according to the vegetation index correlation analysis. Between the reference images and the historical images, the vegetation coverage in the historical images could be obtained. As introduced by Zeng (2004), the specific approach was to use three representations of special features in images from any period: clear and deep water bodies, the densest vegetation, and dry, bare land. The vegetation index Vi1 could then be calculated. In the reference image, the corresponding three representative features could also be found, and their vegetation index Vi could be

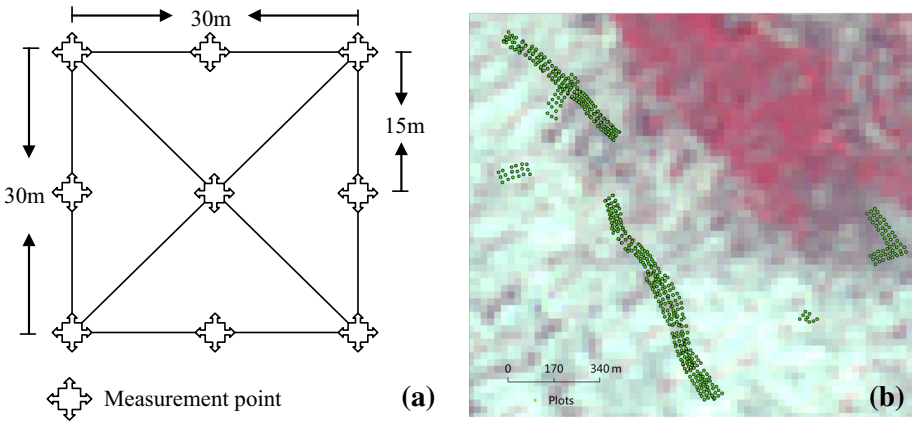

Fig. 2 **a** Measurement points in the plot and **b** spatial distribution of some measured points

calculated by a regression. In this way, we established a quantitative relationship between Vi and Vi1. This relationship was linear: $\mathrm{Vi} = a + b\mathrm{Vi1}$. Thus, the formula $\mathrm{Vc} = \mathrm{f}\,(\mathrm{Vi1})$ was obtained. This method was not only able to estimate the vegetation coverage in any historical period in the study area, but could also apply the vegetation coverage to any pixel.

2.4 Soil wind erosion retrieval method

In the process of obtaining mean Q in the Yuyang sandy area, we arrived at two hypotheses: (1) during spring and early summer, vegetation coverage has an important influence on the wind erosion process in the Yuyang sandy area compared to other factors. We used changes in vegetation coverage to estimate the amount of wind erosion in different land-cover types, although other factors (such as soil wetness, wind speed, and soil texture) could influence the wind erosion process; (2) during recent decades (i.e., from the 1980s to 2000s), the U_{10} was similar to that in 2006 and 2007 on a local scale, and vegetation coverage factors not related to wind conditions were important in controlling the wind erosion process. The mean Q for different types of land cover was therefore considered unchanged, as was the case in 2006 and 2007, so that the average wind speed from 1951 to 2003 was chosen to calculate mean Q, other than the wind speeds in individual years.

The Q on the pixel scale in the Yuyang sandy area during recent decades was computed in several steps. (1) The empirical relationship of vegetation coverage with NDVI was constructed through nonlinear fitting between the observational vegetation coverage of the sample plots in 2006 and 2007 and their corresponding NDVI, retrieved by the TM images in 2005 (see Fig. 3a). Using this relationship and the linear linkage between NDVI in 2005 and in 1986 and 1996, the vegetation coverage of Yuyang on the pixel scale in 1986 and 1996 could be obtained through the NDVI in 1986 and 1996. (2) We calculated the average Q for a year for different types of land cover. During this process, the Q was computed on the basis of observations of q and U_2. The U_2 was transferred from U_{10}. Mean Q was then transferred from Q. (3) With respect to the mean Q and the mean vegetation coverage on different types of land cover, the relationship between mean Q and vegetation coverage was developed (see Fig. 3b). (4) According to this relationship, the mean Q in the sandy area of Yuyang on the pixel scale during recent decades could be estimated by inputting the vegetation coverage for 1986, 1996, and 2005, transferred from the TM images following procedure (2) (see Fig. 3c).

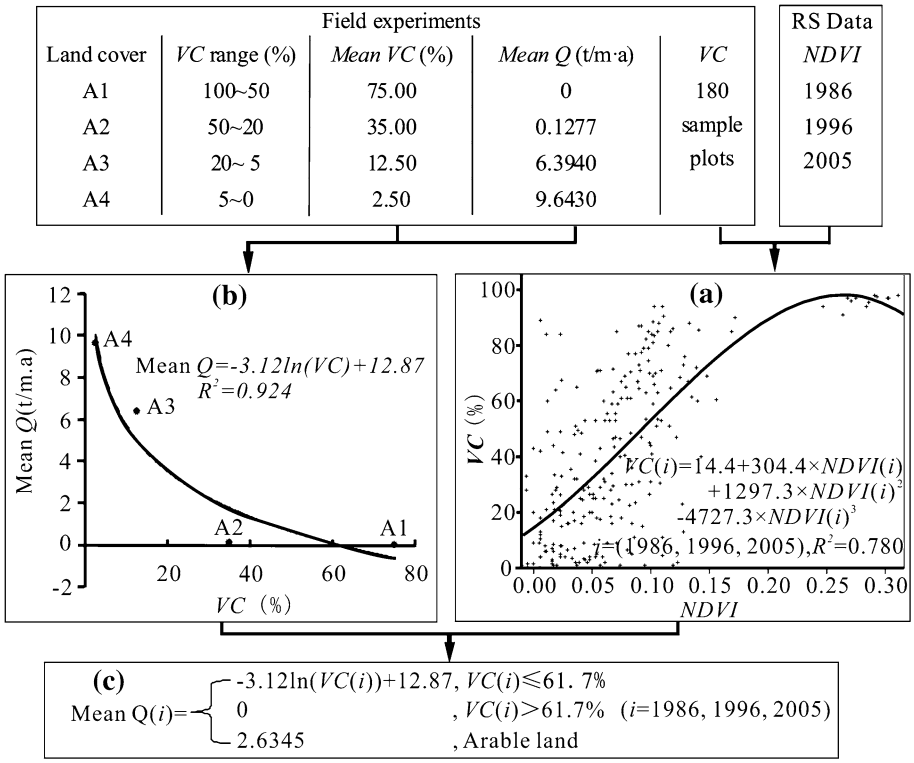

Fig. 3 Framework of the retrieval model for wind erosion on the regional scale

The quantitative relationship between vegetation coverage and mean Q has been the subject of much research and debate in sand kinetics. Measurements indicate that from the fixed dune, semi-fixed dune, and semi-mobile dune to the mobile dune on the surface, the fixed extent declines with each lower level. The sand transport rate increased roughly 1–2 orders of magnitude under the same wind conditions (Liu 1999). Other studies, through wind tunnel experiments and field observation, have demonstrated that the rate of wind-transported sediment increases exponentially with the reduction of vegetation coverage. In quantitative models, Buckley (1987) built a relationship model between vegetation coverage and the wind erosion transport rate by using wind tunnel observation data. Wasson and Nanninga (1986) set up a quadratic exponential relationship model to describe vegetation coverage and the wind sediment transport rate using field observation data. Dong et al. (1996) found that vegetation coverage greater than 60 % produces mild wind erosion and no wind erosion and that 20–60 % results in moderate wind erosion, while less than 20 % produces strong wind erosion. Huang et al. (2001) drew the following conclusions: to ensure that wind erosion transport does not happen in a 12 m × s^{-1} wind, the vegetation coverage must be more than 40 %; to reduce the amount of sand transport significantly at a 20–25 m × s^{-1} extreme wind speed, the vegetation coverage would have to reach a 60–70 % level. These studies have demonstrated a quantitative relationship between vegetation coverage and the q, Q, and mean Q. Having obtained the mean Q for different underlying surfaces and having measured the regional vegetation coverage, we could use regression analysis methods to establish the model for the regional soil erosion inversion.

Table 1 Quantitative relationship between vegetation coverage and mean sediment flux

Surface type	VC range (%)	The average VC (%)	Mean Q ($t \times a^{-1} \times m^{-1}$)
Fixed sand dunes	$100 > VC >= 50$	75.00	0
Semi-fixed sand dunes	$50 > VC >= 21$	35.00	Mean Q_1
Semi-mobile dunes	$20 > VC >= 5$	12.50	Mean Q_2
Mobile dunes	$5 > VC >= 0$	2.50	Mean Q_3

The key to the model was to build a quantitative relationship between mean Q and vegetation coverage, as well as to determine the critical vegetation coverage of wind accumulation. Because the vegetation coverage showed variation that corresponded to the different underlying surfaces, we used the average for the surface vegetation cover state and the corresponding sand transport flux results from Eq. 4. Because wind erosion still occurs at a vegetation cover of 50–60 % in parts of our study region, including the Mu Us Desert (Huang et al. 2001), we assumed that vegetation coverage was 75 % when the mean Q was zero under extremely strong wind conditions. In this case, all the cultivated land pixels were taken that had the same sand flux within the region. Additionally, although not all of the areas were dunes and erodible land, there were lower inter-dunes and high-coverage vegetated areas, but these lands were usually soil deposit areas, and seldom influenced the sand flux. The quantitative relationship between mean Q and vegetation coverage was thus determined to be suitable for a base on which to build the model (Table 1).

By calculating sand transport flux using this method, the complex sand transport process would be simplified to determine the relationship between the underlying surface and sand transport flux. Therefore, if the underlying surface type and its width of sand transport boundary section (extracted from the ground-based remote sensing data) were discovered, we could obtain the equilibrium erosion and deposition and then determine the intensity of erosion and deposition for a certain area. According to this theory, Liu (1999) proposed a regional wind erosion modulus calculation model based on the net sand flux of a given land-use/land-cover type. This model can be described as follows:

$$M = \text{Mean}\, Q \times L \tag{8}$$

where mean Q is the mean annual sand transport flux of a certain underlying surface type. L is the width of the sand transport boundary section, e.g., the width of the underlying surface type.

In this research, we adopted Liu's model to calculate the soil wind erosion modulus in the Yuyang sandy area, based on mean Q at a pixel scale retrieved from remote sensing data. The parameter L is obtained by applying a supervised classification method to remote sensing images, based on underlying surface types in the study area.

3 Results and discussion

3.1 Observed wind erosion

Based on the observations of wind erosion from March to June in 2006 and 2007, we obtained the empirical formulas for q for different land surface types (Table 2).

Table 2 Relationship between wind velocity (V) and sand transporting rate (q) on different land surface types

Location	Land surface type	Empirical formulas for q	Samples
Yuyang sandy area of Mu Us desert	Bare arable land	$q_1 = 3 \times 10^5 \times (0.77u_{10})^{6.2695}$ ($R^2 = 0.88$, $u_{10} \geq 5$ ms^{-1})	15
	Mobile sand dunes	$q_2 = 7.8 \times 10^{-3} \times e^{0.747u_{10}}$ ($R^2 = 0.89$, $u_{10} \geq 5$ ms^{-1})	25
	Low-coverage grassland and semi-mobile dunes	$q_3 = 1.2 \times 10^{-9} \times (0.77u_{10})^{10.874}$ ($R^2 = 0.73$, $u_{10} \geq 6$ ms^{-1})	27
	Bush and mid-coverage grassland and semi-fixed sand dunes	$q_4 = 3.6663 \times 10^{-5} \times (0.77u_{10})^{4.8481}$ ($R^2 = 0.73$, $u_{10} \geq 7$ ms^{-1})	15

where q_i is the average sediment transport rate (kgm^{-1} h^{-1}), and u_{10} is the wind velocity at 10 m above ground (ms^{-1})

Many previously proposed equations for sand transport, such as the mass transport rate expressions given in Greeley and Iversen (1985), suggest that q should essentially be proportional to U^3. However, for all land-cover types, our data indicate that q is a function of u_{10} raised to a power much greater than 3. Therefore, we used the new empirical equations were presented in Table 2 rather than previously proposed formulas.

By analyzing meteorological data, the duration of wind speed over the sand entrainment threshold in different directions was obtained (Table 3). The results show that the mean Q was 9,643 kga^{-1} m^{-1} with mobile dunes, 6,394 kga^{-1} m^{-1} with semi-mobile dunes (low-coverage grassland), 2,634.5 kga^{-1} m^{-1} with bare farmland, 127.7 kga^{-1} m^{-1} with semi-fixed sand dunes (mid-coverage grassland), and 0 kga^{-1} m^{-1} with fixed dunes (high-coverage grassland) during our field survey.

3.2 Vegetation coverage and its changes

Based on the measured vegetation coverage of more than 180 plots, an empirical model was developed using a regression analysis between vegetation coverage and NDVI for 2005 (Eq. 9).

$$\begin{aligned} \mathrm{VC}_{2005} = {} & 14.406 + 304.427 \times \mathrm{NDVI}_{2005} + 1,297.265 \times \mathrm{NDVI}_{2005}^2 \\ & - 4,727.312\mathrm{NDVI}_{2005}^3 (R^2 = 0.78) \end{aligned} \tag{9}$$

According to the relationship of NDVI2005 with NDVI1996 and NDVI1986 (Eq. 10–11), the vegetation coverage in 1986 and 1996 in Yuyang County was obtained (Eq. 12–13). The vegetation coverage for the Yuyang sandy area was then calculated (Fig. 4).

$$\mathrm{NDVI}_{2005} = 0.787 \times \mathrm{NDVI}_{1996} + 0.047 \quad (\mathrm{R}^2 = 0.98) \tag{10}$$

$$\mathrm{NDVI}_{2005} = 0.818 \times \mathrm{NDVI}_{1986} + 0.055 \quad (\mathrm{R}^2 = 0.99) \tag{11}$$

$$\begin{aligned} \mathrm{VC}_{1996} = {} & 14.406 + 304.427 \times (0.787 \times \mathrm{NDVI}_{1996} + 0.047) \\ & + 1297.265 \times (0.787 \times \mathrm{NDVI}_{1996} + 0.047)^2 - 4727.312 \times (0.787 \\ & \times \mathrm{NDVI}_{1996} + 0.047)^3 \quad (R^2 = 0.78) \end{aligned} \tag{12}$$

Table 3 Duration of wind (speed ≥5 ms^{-1}) per year in different directions in Yuyang County (h)

Wind direction	Duration (h) of wind speed exceeding the sand blown speed(≥5 ms^{-1}) per year													Total duration (h)
	5–6	6–7	7–8	8–9	9–10	10–11	11–12	12–13	13–14	14–15	15–16	16–17	≥17	
N	32.92	20.70	11.65	5.66	2.15	1.47	0.23	1.13	0.11	0.11	0.11	0.00	0.00	76.25
NNE	18.10	11.43	5.54	1.92	0.91	1.13	0.23	0.11	0.00	0.00	0.11	0.00	0.00	39.48
NE	7.01	4.41	1.92	0.79	0.34	0.57	0.00	0.11	0.00	0.11	0.00	0.11	0.00	15.39
ENE	4.98	2.94	1.13	0.91	0.00	0.00	0.00	0.11	0.00	0.00	0.00	0.00	0.00	10.07
E	4.86	2.60	0.57	0.79	0.11	0.00	0.11	0.00	0.00	0.00	0.00	0.00	0.00	9.05
ESE	15.61	6.22	1.70	1.02	0.11	0.34	0.00	0.00	0.00	0.00	0.00	0.00	0.00	25.00
SE	57.24	26.13	12.22	7.35	1.24	1.47	0.34	0.00	0.11	0.00	0.00	0.00	0.11	106.23
SSE	113.58	61.66	37.11	16.52	5.88	2.38	0.91	0.57	0.11	0.00	0.00	0.00	0.00	238.71
S	38.92	23.53	11.54	6.22	2.49	1.92	0.11	0.23	0.00	0.00	0.00	0.00	0.00	84.96
SSW	14.82	4.30	2.38	0.91	0.34	0.00	0.11	0.11	0.00	0.00	0.00	0.00	0.00	22.97
SW	7.58	3.05	1.36	0.57	0.00	0.11	0.00	0.00	0.11	0.00	0.00	0.00	0.00	12.78
WSW	9.28	5.54	3.05	1.70	0.91	0.91	0.11	0.23	0.00	0.00	0.00	0.00	0.00	21.72
W	10.07	8.03	3.73	2.49	1.02	1.24	0.34	0.45	0.34	0.23	0.00	0.00	0.11	28.06
WNW	23.76	15.27	13.24	9.84	6.45	5.54	0.91	1.70	0.79	0.45	0.45	0.34	0.34	79.08
NW	46.72	36.77	24.32	19.35	9.05	8.94	1.58	4.07	0.79	0.91	0.91	0.11	0.34	153.86
NNW	70.14	45.59	38.01	23.53	11.77	9.62	2.04	2.94	1.02	0.91	0.45	0.34	0.45	206.80
Total	475.60	278.19	169.47	99.56	42.76	35.64	7.01	11.77	3.39	2.72	2.04	0.91	1.36	1,130.41

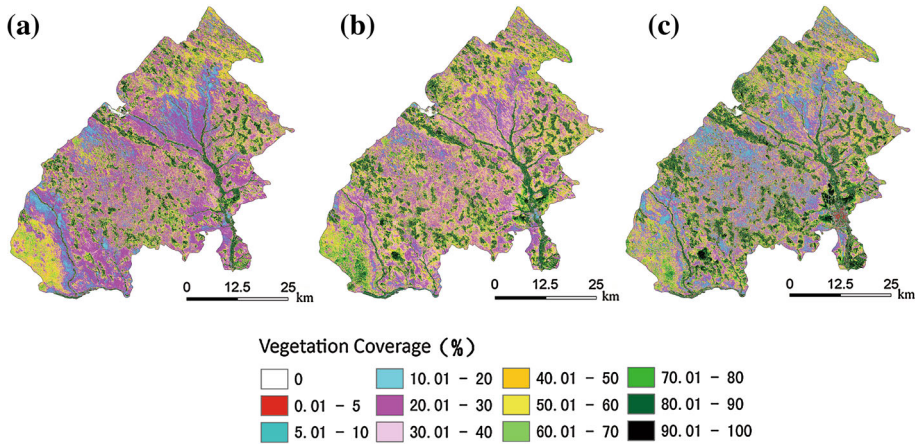

Fig. 4 Vegetation cover rate for the Yuyang sandy area (**a** 1986, **b** 1996, **c** 2005)

$$\begin{aligned} \mathrm{VC}_{1986} &= 14.406 + 304.427 \times (0.818 \times \mathrm{NDVI}_{1986} + 0.055) \\ &\quad + 1297.265 \times (0.818 \times \mathrm{NDVI}_{1986} + 0.055)^2 - 4727.312 \\ &\quad \times (0.818 \times \mathrm{NDVI}_{1986} + 0.055)^3 \quad (R^2 = 0.78) \end{aligned} \tag{13}$$

Vegetation coverage changes reflect the corresponding wind erosion risk of land surfaces. We employed an area-weighted computation method to calculate the average vegetation coverage at the sandy area of Yuyang County, which was 42.39, 48.07, and 48.03 % for 1986, 1996, and 2005, respectively, reflecting an increment in vegetation coverage and the recovery of the ecological environment in the Yuyang sandy area. We also compared the changes in area during 1986, 1996, and 2005 according to the different vegetation coverage levels in the Yuyang sandy area. The results show that during the last several decades, areas with vegetation coverage that exceeds 50 % have increased. Areas with vegetation coverage of 30–50 % increased from 1986 to 1996 and then decreased from 1996 to 2005. In contrast, the areas with vegetation coverage of 10–30 % showed a decreasing trend over the last decades, with the percentage of the area that was sandy land dropping from 38.68 % in 1986 to 21.57 % in 1996 and 28.34 % in 2005.

These results differ from results of previous studies. Wu (2001), Runnström (2003), and Wu and Ci (1998, 2002) reported rapid rehabilitation in the Mu Us Desert after the mid-1980s. Specifically, in the eastern Mu Us region, trends in remotely sensed vegetation greenness and changes in mobile dune areas inferred from sequential Landsat images indicate widespread dune stabilization, with active dunes decreasing from 34 % in 1978 to 30 % in 2002 (Mason et al. 2008). However, our results indicate that dunes with vegetation coverage of less than 20 % increased dramatically in 2005 compared to 1986 and 1996 and that mobile dunes where vegetation coverage is less than 10 % were still expanding. Additionally, our data show that the percentage of sandy land area in Yuyang has changed from 28.9 % in 1986 to 36.34 % in 1996 and 40.37 % in 2005. Of course, this study focuses on just the Yuyang sandy area, which is a small portion of the Mu Us Desert, so the results cannot represent the entire desert. Our results show that the Yuyang sandy area has a trend of increasing overall vegetation coverage, however, but that the coverage has

decreased at a local scale, with the overall effect that there are increased areas of exposed land surface that are prone to wind erosion.

In addition to its impact on global climate change, human activity is most likely the main cause of land-use/land-cover change in the study area. Pilot studies, such as Zhang et al. (2008), report that the total sandy area in Yulin (with a study area that is the same as ours) increased continuously from 1960 to 2006. This suggests that desertification in the Yulin area is probably still increasing and is potentially quite serious. There are debates on the causes and driving forces of desertification in the region (Wang et al. 2005b, 2006); most desert areas with vegetated dune systems in arid and semiarid northern China, however, are used for farming or grazing (Mason et al. 2008). Activities such as over-reclamation, over-grazing, and over-cutting (Chen et al. 1994; Wang and Zhu 2001; Wu 2001; Runnström 2003; Wu and Ci 1998, 2002; Zha et al. 2008; Zhang et al. 2008; D'Odorico et al. 2013) could thus significantly affect land cover and lead to desertification in the area. On the other hand, continued growth in mining and urbanization has also had an adverse impact on the landscape. At present, regional economic development is in direct conflict with the protection of vegetation cover. The conflict has caused damage to land resources and the fragmentation of the landscape, accompanied by desertification (Zha et al. 2008). Moreover, these activities will eventually lead to increased wind erosion. More attention should thus be directed at minimizing the negative impact of human activities, particularly economic development, on land use/cover.

3.3 Quantitative retrieval of wind erosion

Based on our data, we derived an empirical model showing the relationship between observational wind transport flux and vegetation coverage using a regression analysis, on the sample fields in the sandy land of Yuyang (Fig. 3a, Eq. 14).

$$\text{Mean } Q = -3.1242 \times \text{Ln}(\text{VC}) + 12.87 (R^2 = 0.924) \tag{14}$$

where mean Q represents wind transport flux ($\text{ta}^{-1}\ \text{m}^{-1}$) for a given value of vegetation coverage and the vegetation coverage is limited to less than 61.7 %. VC stands for vegetation coverage.

Wiggs et al. (1995) pointed out that dune sand transport is significantly inhibited or prevented by vegetation cover greater than 40 % in regions like the southwestern Kalahari Desert, but wind erosion still occurs at a vegetation cover of 40–50 % in parts of our study region (Huang et al. 2001). Dong et al. (1996) found that when vegetation coverage is more than 60 %, wind erosion is slight or that no erosion might occur. However, we encountered a threshold of 61.7 % in our field data, which means that when vegetation coverage exceeds 61.7 %, the saltation of soil particles stops and the soil particles are stacked. This threshold is very close to that verified by a field survey conducted in the Mu Us Desert (Huang et al. 2001) and by related wind tunnel experiments (Dong et al. 1996). This supports the proposed model's ability to reflect the relationship between the sand transport flux and vegetation coverage. Meanwhile, the RMSE of 0.84, based on simulated and measured values, indicates that the model has acceptable accuracy. Following Eq. 14, we obtained the wind erosion quantity at pixel scale in 1986, 1996, and 2005, respectively (Fig. 5).

According to our data and model, the soil wind erosion modulus is 1,673.18, 1,568.10, and 1,685.04 $\text{ta}^{-1}\ (\text{km}^2)^{-1}$ in 1986, 1996, and 2005, respectively, and average 1,642.11 $\text{ta}^{-1}\ (\text{km}^2)^{-1}$. This is in line with the findings of Liu (1999) in the Mu Us Desert

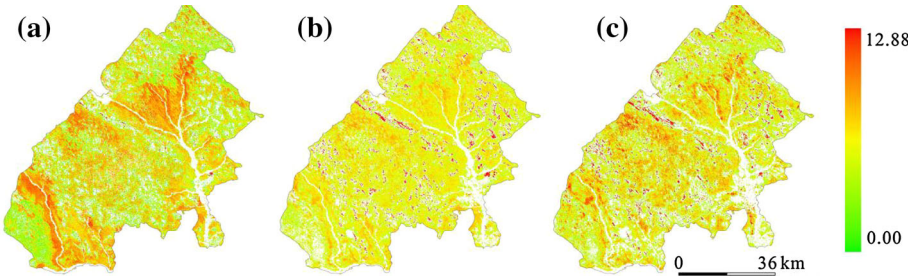

Fig. 5 Sand flux of wind erosion in Yuyang sandy area (**a** 1986, **b** 1996, **c** 2005, unit: t/m·a)

of 1,600 ta^{-1} $(km^2)^{-1}$ and is slightly lower than the 1,887.27 ta^{-1} $(km^2)^{-1}$ obtained by Dong (1998) in Shenmu County (adjacent to Yuyang County). The results confirm that our model, which uses remote sensing data in conjunction with a field survey to quantitatively retrieve data on wind erosion at a regional scale, is feasible and reliable.

Moreover, compared to prior proposed models, the model is simple, yet it has the ability to output dynamic wind erosion data at pixel scale. Many factors have been studied that can affect wind erosion, primarily related to wind speed, soil moisture, soil texture, vegetation cover, and human activity (Woodruff and Siddoway 1965; Hagen 1991; Hagen et al. 1995; Dong et al. 1996; Fryrear et al. 1998; Shao et al. 1996; Lu and Shao 2001; Gregory et al. 2004; Coen et al. 2004). However, the models used in these studies do not necessarily perform better than our model, which might be explained by the fact that the relationship between wind erosion with the model variables remains unclear or is very hard to determine (Woodruff and Siddoway 1965; Dong 1998). For this reason, collecting sufficient empirical data of adequate quality and finding the most sensitive factor may be more helpful than using multiple factors to build a regional wind erosion model (Stroosnijder 2005). Among the factors, vegetation has been widely acknowledged as the most sensitive factor because of its importance when soil and climate are similar over an area (such as our study area) or vary slowly. On the one hand, vegetation changes the surface roughness and wind erosion intensity (Wasson and Nanninga 1986; Buckley 1987; Wiggs et al. 1995; Dong 1998; Lancaster and Baas 1998; Huang et al. 2001). On the other hand, however, vegetation is a condition most easily changed by human activity, and it often thus exhibits great spatial variability.

Vegetation coverage has been included as a factor in some regional wind erosion models (Dong 1998; Liu 1999; Shao et al. 1996). Due to the complexity of his model, Dong (1998) used vegetation data for a single type of land erosion as an input. This greatly reduced the spatial accuracy of the model. This is because even within a single land type, vegetation coverage varies significantly in space. Liu (1999) also did not consider the variability of vegetation coverage in space. These models were thus unable to take full advantage of the high spatial resolution of remote sensing data. The quality of the database, including vegetation coverage, thus still needs improvement (Shao et al. 1996). This study attempted to solve the deficiencies in this respect. Once the wind erosion empirical model is established through field observations, as long as there are new remote sensing data, a dynamic estimate of soil erosion at pixel scale can be achieved.

Another advantage of the proposed model relates to pixel scale-based large area erosion estimates. Many wind erosion models have been applied successfully to obtain accurate wind erosion rates, including the wind erosion equation (WEQ) (Woodruff and Siddoway

1965), the revised wind erosion equation (RWEQ) (Fryrear et al. 1998), the wind erosion prediction system (WEPS) (Hagen 1991; Hagen et al. 1995), the Texas Tech Erosion Analysis Model (TEAM) (Gregory et al. 2004), and the integrated wind erosion modeling system (IWEMS) (Shao et al. 1996; Lu and Shao 2001). However, the WEQ, RWEQ, and TEAM models were developed on the basis of field observations, and it is difficult to extend these field observations beyond the regions where they were developed. In addition, the WEPS model is primarily functional on the point scale and cannot meet research needs for larger regional wind erosion estimations (Coen et al. 2004). In general, the biggest shortcoming of these models is that they cannot be applied in regional dynamic wind soil erosion monitoring.

Although some studies have developed models based on remote sensing data (Chappell 1998; Gabor and Jozsef 1998), they have either been exclusively suitable for farmland (Chappell 1998) or did not integrate field observations into the model (Gabor and Jozsef 1998). Remote sensing can provide direct measurements and measurements of inputs for erosion models via the empirical relation between erosion and reflection. Few studies, however, have measured wind erosion on a large spatial scale using remote sensing data combined with field survey erosion data to providing inputs for the models, owing to a dearth in sufficient empirical data of adequate quality (Stroosnijder 2005). There remains little research on regional wind erosion measurement through field surveys and remote sensing data. This paper is only a small step, but we hope to enable deeper related research in the future.

4 Conclusions

We developed a model by which we can quantitatively retrieve soil wind erosion on a regional scale from remote sensing data and field surveys. The model was constructed using the following steps: (1) Sample plots were selected, and their vegetation coverage and soil erosion sand transport flux and NDVI were investigated; (2) the relationship between soil erosion and vegetation coverage, as well as the relationship between vegetation coverage and NDVI, was constructed by nonlinear fitting; and (3) the estimation of regional soil erosion was obtained according to the relationship derived above, using the NDVI from remote sensing data, which is dynamic and could be rapidly observed.

The study used a field survey and wind speed data collected over several years to estimate a sand transport rate in the Yuyang sandy area, and then determined the sand flux. The sand transport flux was 9,643, 6,394, 2,634.5, and 127.7 kga^{-1} m^{-1} for mobile dunes, semi-mobile dunes, arable land, and semi-fixed sand dunes, respectively. The vegetation coverage of the area was measured; average vegetation coverage was 42.39, 48.07, and 48.03 % in 1986, 1996, and 2005, respectively. Finally, on the basis of the relationship between vegetation coverage and soil erosion transport flux, the volume of regional soil erosion was calculated. The soil erosion modulus in the sandy area of Yuyang was 1,673.18 ta^{-1} $(km^2)^{-1}$ in 1986, 1,568.10 ta^{-1} $(km^2)^{-1}$ in 1996, and 1,685.04 ta^{-1} $(km^2)^{-1}$ in 2005. The increased regional vegetation coverage has not prevented soil wind erosion in the Yuyang sandy area.

Although our research implies that the model presented here can provide a dynamic and high-precision estimation of wind soil erosion, many aspects of the model could be improved. These improvements are currently beyond the scope of this study, however. Shortcomings that could be addressed in future studies include: (1) The type of underlying ground was not optimally factored into the measurement of soil erosion, and the

observation time for the field survey was short; (2) the observations of sand transport flux might not have exactly coincided with the real value of sand transport flux because the wind velocity used for the study was the mean value over the previous 6 h, so the value might not represent the real-time value of the wind velocity; and (3) the model did not consider other variables that play important roles in wind erosion, such as relative humidity and soil wetness. Although field observations of wind erosion reflect the influence of soil moisture and other factors on wind erosion to a certain degree, soil moisture needs to be considered in order to improve the accuracy of model prediction.

Acknowledgments This research is financially supported by the National Basic Research Program of China (973 Program) (No. 2012CB955403), NSF project (No. 41321001). We would like to thank Joseph A. Mason for his valuable suggestions for improving the study. Sincere thanks should also be given to the editor and four anonymous reviewers for their constructive comments and suggestions that greatly helped to improve the quality of this article.

References

Ackerman S (1997) Remote sensing aerosols using satellite infrared observations. J Geophys Res 102:17069–17079

Bagnold RA (1941) The physics of blown sand and desert dunes. Methuen and Co., London

Buckley R (1987) The effect of sparse vegetation on the transport of dune sand by wind. Nature 325:426–428

Chappell A (1998) Using remote sensing and geostatistics to map 137Cs-derived net soil flux in the south-west Niger. J Arid Environ 39:441–455

Chen WN, Dong GR, Dong ZB (1994) Achievements and needs of studies on wind erosion in Northern China. Adv Earth Sci 9:6–12 (in Chinese with English abstract)

Chen YH, Shi PJ, Li XB, Chen J, Li J (2006) A combined approach for estimating vegetation cover in urban/suburban environments from remotely sensed data. Comput Geosci 32:1299–1309

Coen GM, Tatarko J, Martin TC, Cannon KR, Goddard TW, Sweetland NJ (2004) A method for using WEPS to map wind erosion risk of Alberta soils. Environ Model Softw 19(2):185–189

D'Odorico P, Bhattachan A, Davis KF, Ravi S, Runyan CW (2013) Global desertification: drivers and feedbacks. Adv Water Resour 51:326–344

Dong ZB (1998) Establishing statistic model of wind erosion on small watershed basis. Bull Soil Water Conserv 18:55–62 (in Chinese with English abstract)

Dong ZB, Chen WN, Chen GT, Li ZS, Yang ZT (1996) Influences of vegetation cover on the wind erosion of sandy soil. Acta Scientiae Circumstantiae 16:437–443 (in Chinese with English abstract)

Dong ZB, Wang XM, Liu LY (2000) Wind erosion in arid and semiarid China: an overview. J Soil Water Conserv 55:439–444

Fryrear DW, Saleh A, Bilbro JD, Schomberg HM, Stout JE, Zobeck TM (1998) Revised wind erosion equation (RWEQ). Wind erosion and water conservation research unit, USDA-ARS, Southern Plains area cropping systems research laboratory. Tech Bull 1. http://www.csrl.ars.usda.gov/wewc/rweq.htm

Gabor M, Jozsef S (1998) Assessment of wind erosion risk on the agricultural area of the southern part of Hungary. J Hazard Mater 61:139–153

GLP (2005) Global land project—science plan and implementation strategy [IGBP (International Geosphere Biosphere Program) Report No. 53/International Human Dimensions Programme Report No. 19, IGBP Secretariat, Stockholm]. www.globallandproject.org/documents.shtml

Greeley R, Iversen J (1985) Wind as a geological process on Earth, Mars, Venus and Titan. Cambridge University Press, London

Gregory JM, Wilson GR, Singh UB, Darwish MM (2004) TEAM: integrated, process-based wind-erosion model. Environ Model Softw 19:205–221

Hagen LJ (1991) A wind erosion prediction system to meet the user's need. J Soil Water Conserv 46(2):106–111

Hagen LJ, Wagner LE, Tatarko J (1995) Wind erosion prediction system (WEPS): introduction. In: Wind erosion prediction system technical description. Proceedings of WEPP/WEPS symposium, Des Moines, IA. Soil and Water Conservation Society, Ankeny, IA

Huang FX, Niu HS, Wang MX, Wang YS (2001) The relationship between vegetation cover and sand transport flux at Mu Us sandland. Acta Geogr Sin 56:700–710 (in Chinese with English abstract)
Kassas M (1995) Desertification: a general review. J Arid Environ 30:115–128
Kuhlman H (1958) Quantitative measurements of Aeolian sand transport. Geografisk Tidsskrift 57:51–74
Lancaster N, Baas A (1998) Influence of vegetation cover on sand transport by wind: field studies at Owens Lake, California. Earth Surf Process Land 23(1):69–82
Liu LY (1999) The quantify and intensity of regional Aeolian sand erosion and deposition: the case of Shanxi-Shaanxi-Neimonggol region. Acta Geogr Sin 54:59–68 (in Chinese with English abstract)
Lu H, Shao YP (2001) Toward quantitative prediction of dust storms: an integrated wind erosion modeling system and its applications. Environ Model Softw 16:233–249
Mason JA, Swinehart JB, Lu HY, Miao XD, Cha P, Zhou YL (2008) Limited change in dune mobility in response to a large decrease in wind power in semi-arid northern China since the 1970s. Geomorphology 102:351–363
MEA (Millennium Ecosystem Assessment) (2005) Ecosystems and human well-being: desertification synthesis. World Resources Institute, Washington
Owen PR (1964) Saltation of uniform sand grains in air. J Fluid Mech 20:225–242
Prospero JM, Ginoux P, Torres O, Nicholson SE, Gill TE (2002) Environmental characterization of global sources of atmospheric soil dust identified with the NIMBUS 7 Total Ozone Mapping Spectrometer (TOMS) absorbing aerosol product. Rev Geophys 40:2–31
Reiche M, Funk R, Zhang ZD, Hoffmann C, Reiche J, Wehrhan M, Li Y, Sommer M (2012) Application of satellite remote sensing for mapping wind erosion risk and dust emission-deposition in Inner Mongolia grassland, China. Grassl Sci 58(1):8–19
Reynolds JF, Smith DM, Lambin EF, Turner BL, Mortimore M, Batterbury SP, Downing TE, Dowlatabadi H, Fernández RJ, Herrick JE, Huber-Sannwald E, Jiang H, Leemans R, Lynam T, Maestre FT, Ayarza M, Walker B (2007) Global desertification: building a science for dryland development. Science 316:847–851
Runnström MC (2003) Rangeland development of the Mu Us sandy land in semiarid China: an analysis using Landsat and NOAA remote sensing data. Land Degrad Dev 14:189–202
Shao YP, Raupach MR, Leys JF (1996) A model for prediction aeolian sand drift and dust entrainment on scales form paddock to region. Aust J Soil Res 34:309–342
Stroosnijder L (2005) Measurement of erosion: is it possible? Catena 64:162–173
Toy TJ, Foster GR, Renard KG (2002) Soil erosion: processes, prediction, measurement and control. Wiley, New York
Wang T, Zhu ZD (2001) Some problems of desertification in northern China. Quat Sci 21:56–65 (in Chinese with English abstract)
Wang XM, Chen FH, Dong ZB, Xia DS (2005a) Evolution of the southern Mu Us Desert in North China over the past 50 years: an analysis using proxies of human activity and climate parameters. Land Degrad Dev 16:351–366
Wang XM, Dong ZB, Yan P, Zhang JW, Qian GQ (2005b) Wind energy environments and dunefield activity in the Chinese deserts. Geomorphology 65:33–48
Wang XM, Chen FH, Dong ZB (2006) The relative role of climatic and human factors in desertification in semi-arid China. Glob Environ Change (Part A) 16:48–57
Wang XM, Chen FH, Eerdun HS, Li JC (2008) Desertification in China: an assessment. Earth Sci Rev 88:188–206
Wang XX, Liu TX, Li FL, Gao RZ, Yang XM, Duan LM, Luo YY, Li R (2014) Simulated soil erosion from a semiarid typical steppe watershed using an integrated aeolian and fluvial prediction model. Hydrol Process 28(2):325–340
Wasson RJ, Nanninga PM (1986) Estimation wind transport of sand on vegetated surface. Earth Surf Process Land 11:505–514
Wiggs GFS, Thomas DSG, Bullard JE (1995) Dune mobility and vegetation cover in the Southwest Kalahari Desert. Earth Surf Process Land 20:515–529
Woodruff NP, Siddoway FH (1965) A wind erosion equation. Soil Sci Soc Am Process 29:602–608
Wu Z (1987) Aeolian geomorphology. Science Press, Beijing (in Chinese)
Wu W (2001) Study on processes of desertification in Mu Us Sandy Land for last 50 years, China. J Desert Res 21:164–169 (in Chinese with English abstract)
Wu B, Ci LJ (1998) Causes and development stages of desertification in the Mu Us Sandland. Chin Sci Bull 43:2437–2440 (in Chinese with English abstract)
Wu B, Ci LJ (2002) Landscape change and desertification development in the Mu Us Sandland, Northern China. J Arid Environ 50:429–444

Xie YH, Yue YJ, Wang JA (2008) Vegetation identification using combined object-oriented and pixel based classification method. In: International conference on informational technology and environmental system science, 2008/5/15-2008/5/17, Jiaozuo, China, pp 354–358

Xiong LY, Li HP, Zhuang DF (2002) Discuss on quantitative method study of sand-dust information using MODIS data. Prog Geogr 21:327–332 (in Chinese with English abstract)

Yan H, Wang CY, Niu Z, Zhang YP (2002) Remote sensing study of track sand source areas of eastern Asian dust. Prog Geogr 21:90–94 (in Chinese with English abstract)

Zeng ZY (2004) Research on computer classification of satellite images and application in geoscience. Science Press, Beijing (in Chinese)

Zha Y, Liu YS, Deng XZ (2008) A landscape approach to quantifying land cover changes in Yulin, Northwest China. Environ Monit Assess 138:139–147

Zhang GP, Zhang ZX, Liu JY (2002) Spatial changes of wind erosion-caused landscapes and their relation with wind field in China. J Geog Sci 2:30–39

Zhang YZ, Chen ZY, Zhu BQ, Luo XY, Guan YN, Guo S, Nie YP (2008) Land desertification monitoring and assessment in Yulin of Northwest China using remote sensing and geographic information systems (GIS). Environ Monit Assess 147:327–337

Zheng XJ, Lu WJ, Luo JN (2001) Research on the dust storm monitoring using multichannel meteorological satellite data. J Remote Sens 5:300–305 (in Chinese with English abstract)

Zhou Q, Robson M, Pilesjo P (1998) On the ground estimation of vegetation cover in Australian rangelands. Int J Remote Sens 9:1815–1820

Zhu ZD, Chen GT (1994) Sandy desertification in China. Science Press, Beijing (in Chinese)

Zhu ZD, Wu Z, Liu S, Di XM (1980) An introduction to Chinese desert. Science Press, Beijing (in Chinese)

Zobeck TM, Sterk G, Funk R, Rajot JL, Stout JE, Van Pelt RS (2003) Measurements and data analysis methods for field-scale wind erosion studies and model validation. Earth Surf Process Land 28:1163–11881